Molecular Dynamics Study of Thermal Rectification in Graphene Nanoribbons

Jiuning Hu[1*] · Xiulin Ruan[2] · Yong P. Chen[3#]

[1]School of Electrical and Computer Engineering and Birck Nanotechnology Center, Purdue University, West Lafayette, Indiana 47907, USA
[2]School of Mechanical Engineering and Birck Nanotechnology Center, Purdue University, West Lafayette, Indiana47907, USA
[3]Department of Physics, School of Electrical and Computer Engineering and Birck Nanotechnology Center, Purdue University, West Lafayette, Indiana 47907, USA

[*]E-mail: hu49@purdue.edu, Tel: 765-496-3059, Fax: 765-494-0706
[#]E-mail: yongchen@purdue.edu, Tel: 765-494-0947, Fax: 765-494-0706

Abstract We have used classical molecular dynamics based on the Brenner potential and Nosé-Hoover thermostat to study the thermal conductivity and thermal rectification of graphene nanoribbons. We found appreciable thermal rectification effect in triangular and trapezoid nanoribbons. The thermal rectification factor is over 20% even for 23 nm long monolayer triangular nanoribbons. The thermal rectification in graphene nanoribbons may enable novel nanoscale heat management and information processing using phonons.

Keywords Molecular dynamics · Thermal conductivity · Thermal rectification · Graphene nanoribbons

1 Introduction

Graphene, an atomic monolayer of graphite in ab-plane with sp^2 carbon-carbon bonding and honeycomb lattice structure, has been paid tremendous attention since its first experimental isolation in 2004 [1]. Graphene exhibits unusual electronic properties, such as massless Dirac fermions and anomalous quantum Hall effect [2]. In addition, graphene also shows unique thermal and mechanical properties. It has been experimentally demonstrated that graphene has very high thermal conductivity of 3000-5000 W/K-m [3, 4], among materials with the highest thermal conductivities, such as diamond and carbon nanotubes (CNTs). The strong covalent carbon-carbon bonding in graphene contributes dominantly to the thermal conduction whereas the contribution from the electrons is negligible [4] in typical experimental temperatures. This covalent bond also makes graphene one of the strongest materials in the world [5]. Due to those properties, graphene is considered as one of the most versatile materials for future nanoelectronics. Many important devices made from graphene are composed of graphene nanoribbons (GNRs), which are narrow graphene strips of few or tens of nanometers in size. As the fundamental elements in graphene based nanoelectronics, many properties of GNRs can be tuned by their size and edge chirality. For example, both theoretical calculation [6] and experimental demonstration [7] showed that the energy gap of GNRs depends on their width. The thermal properties of GNRs are also of great interests for fundamental physics and potential applications. Recent theoretical studies showed that the thermal conductivity of GNRs depends on their edge chiralities [8, 9]. The effect of thermal rectification (TR), in which the thermal conductivity in one direction is different from that in the opposite direction, is shown in asymmetric GNRs of triangular shape [8, 10]. The chirality dependence of thermal conductivity and TR of asymmetric GNRs may by applied in future nanoscale energy conversion and harvesting devices or in the phonon based logic and computational devices [11-14].

In this work, we used classical molecular dynamics (MD) to study the thermal rectification of trapezoid-shaped GNRs and triangle-shaped GNRs in single or double-layer graphene. We also calculated the size dependence of the thermal rectification of GNRs.

2 Simulation method: classical molecular dynamics

We have used classical molecular dynamics based on Brenner potential [15] to study the thermal transport in GNRs. Brenner potential is widely used in hydrocarbon system. The anharmonic terms of inter-carbon interaction, essential to the nonlinear thermal effect such as finite thermal conductivity and thermal rectification, is automatically embedded in the Brenner potential. The typical GNRs we used in this study is shown in Fig. 1. The atoms denoted by left-pointing and right-pointing triangles at two ends of GNRs are put in the Nosé-Hoover thermostats [16, 17] at different temperatures T_L and T_R (the average temperature is $T=(T_L+T_R)/2$). The equations of motion for the atoms in the Nosé-Hoover thermostats are:

$$\frac{d}{dt}p_i = F_i - \gamma p_i, \frac{d}{dt}\gamma = \frac{1}{\tau^2}\left[\frac{T(t)}{T_0} - 1\right], T(t) = \frac{2}{3Nk_B}\sum_i \frac{p_i^2}{2m} \qquad (1)$$

where the subscript i runs over all the atoms in the thermostat, p_i is the momentum of the i-th atom, F_i is the total force acting on the i-th atom, γ and τ are the dynamic parameter and relaxation time of the thermostat, $T(t)$ is the instant temperature of the thermostat at time t, T_0 ($=T_L$ or T_R) is the set temperature of the thermostat, N is the number of atoms in the thermostat, k_B is the Boltzmann constant and m is the mass of the carbon atom. The atoms denoted by circles are obeying the Newton's law of motion:

$$\frac{d}{dt}p_j = F_j \qquad (2)$$

where j runs over all the atoms denoted by circles. The atoms denoted by squares are fixed to avoid the spurious global rotation of GNRs [18]. The temperature difference at the two ends of GNRs creates a temperature gradient and the corresponding thermal current along the temperature gradient. According to Fourier's law, the thermal conductivity can be calculated from the temperature gradient, thermal current and size of GNRs. In all of the following simulations the temperature has been corrected according to the Debye model by considering the phonon occupation number. The details of the MD simulation including the quantum correction of temperature can be found elsewhere [8, 19].

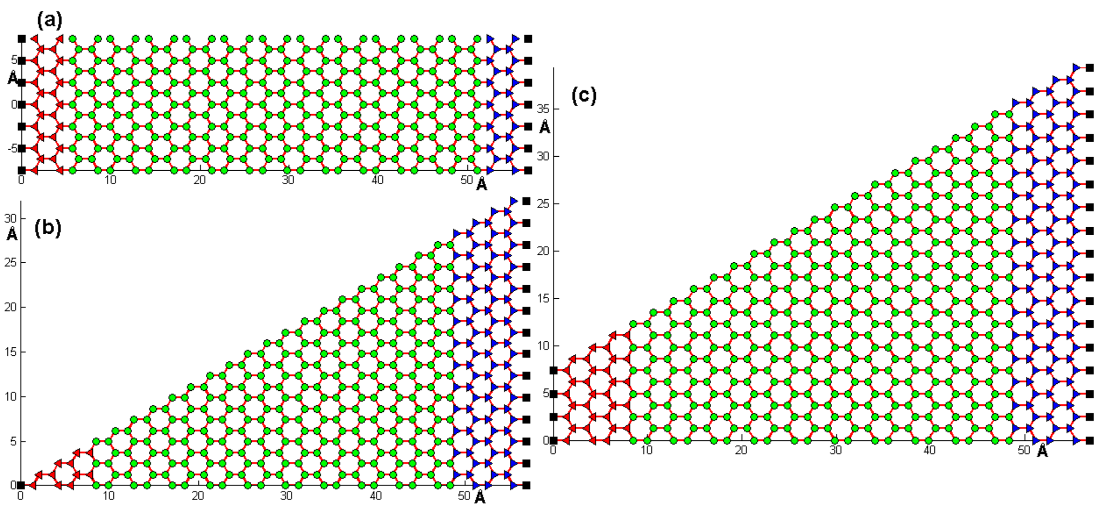

Fig. 1 Structures of GNRs in this study: (a) rectangle, (b) triangle and (c) trapezoid.

3 Thermal rectification in GNRs

For the asymmetric GNRs (e.g., triangular and trapezoid GNRs), the thermal conductivity from the narrower (N) to the wider (W) end and from the wider to the narrower end are denoted by $\kappa_{N\to W}$ and $\kappa_{W\to N}$ respectively. The thermal rectification factor is defined as $\eta=(\kappa_{N\to W}-\kappa_{W\to N})/\kappa_{W\to N}$. In this paper we discuss the thermal rectification of double layer triangular and monolayer trapezoid GNRs and compare the results with the case for monolayer triangular GNRs we studied previously [8]. We also studied the size dependence of the thermal rectification factor for the monolayer triangular GNR as shaped in Fig. 1(b). The simulation results for double layer triangular and monolayer trapezoid GNRs are shown in Fig. 2. The double layer triangular GNR consists of two AB-stacked monolayer triangular GNRs as shown in Fig. 1 (b). Compared with the monolayer triangle GNR (solid lines) of the same size, the double layer triangle GNR (dashed line) has larger thermal conductivity. The enhanced thermal conductivity of the double layer GNR probably comes from the interlayer interaction which can generate several new phonon modes, such as the out-of-plane motion of those two layers with 180° out of phase and the in-plane motion of atoms in two layers moving 180° out of phase, corresponding to the new optical dispersion branches of phonons. Those new phonon modes can contribute to the thermal conduction and thus increase the thermal conductivity. The trapezoid GNRs (Fig. 1c and dash-dotted lines in Fig. 2) have higher thermal conductivity than triangular GNRs (Fig. 1b and solid lines in Fig. 2), possible due to a combination of the geometry and size dependence of thermal conductivity [8]. For the symmetric rectangular GNR of Fig. 1(a), the thermal conductivity from the left (L) to the right (R) end is almost the same as that from the right to the left end, as shown in the dotted lines of Fig. 2 (the small difference is probably from the numerical uncertainty and fluctuations related to MD simulation). The temperature dependence of the thermal conductivity of the rectangular or trapezoidal GNRs is found to be similar to that of the rectangular GNRs.

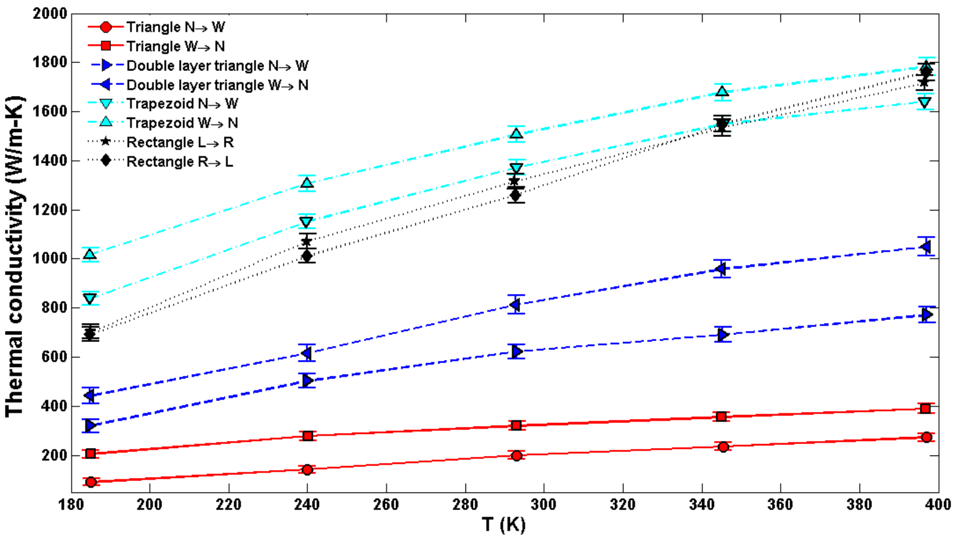

Fig. 2 Thermal rectification of GNRs. The shape and size of the GNRs are specified in Fig. 1.

In Fig. 3, the TR factor as a function of temperature is calculated from the corresponding pair of lines in Fig. 2. For the symmetric rectangular GNR, the TR factor is consistent with zero within the MD uncertainty. For the other asymmetric GNRs, the TR factor is always larger than zero and reach as higher as 120% for the monolayer triangular GNR at T=180 K. The monolayer triangular (solid line) GNR has larger TR factor than the double layer triangular GNR, which has yet larger TR factor than the trapezoid GNR.

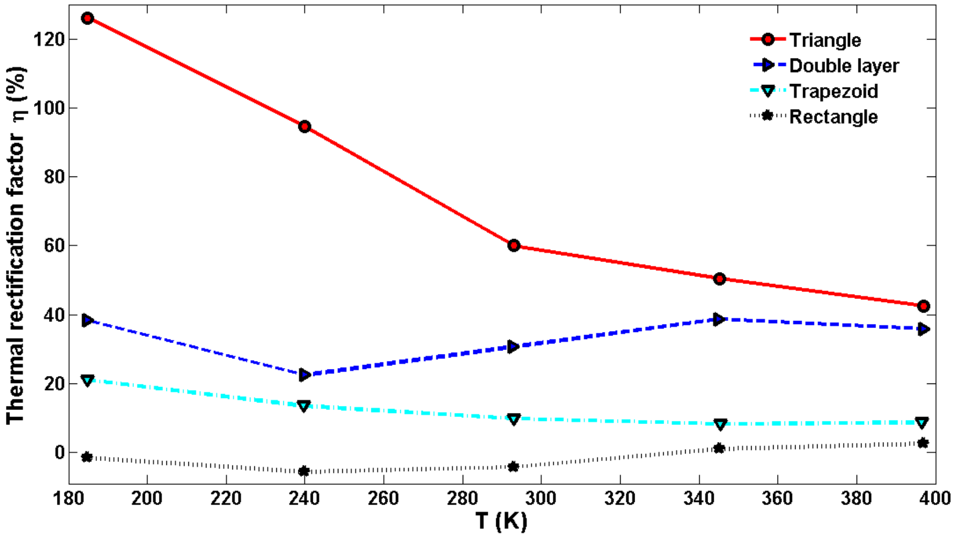

Fig. 3 Thermal rectification factor.

In Fig. 4, we show the size dependence of the thermal rectification factor for monolayer triangular GNR in Fig. 1(b) of perfect (solid line) and rough (dashed line) edges. The atoms at the bottom and hypotenuse edges of various sized triangular GNRs are removed with constant line density of about one vacancy per 1.5 nm to create edge roughness. The thermal rectification factor of perfect triangular GNRs decreases with increase of the size, but is still as large as 25% for GNRs of up to 23 nm long. The size dependence of the thermal rectification factor of rough edged triangular (dashed line in Figure 4(b)) GNRs shows a different behavior from that of perfect GNRs, but it appears that the thermal rectification factor converges to around 30% as we increase the size of both the perfect and rough-edge triangular GNRs.

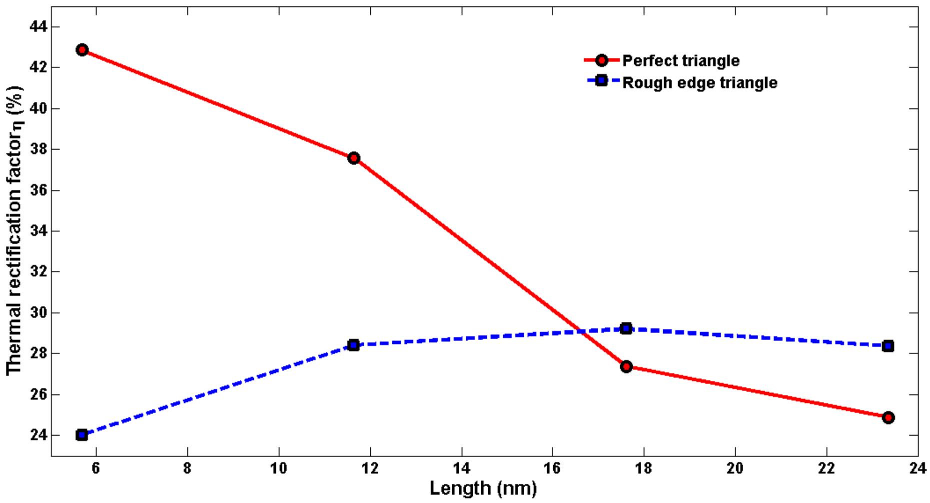

Fig. 4 Size dependence of thermal rectification factor for perfect and roughed edge triangular GNRs.

6 Conclusions

In summary, we have studied thermal transport properties of GNRs using classical MD simulation. The asymmetric triangular and trapezoid GNRs show considerable thermal rectification effect and the size dependence of thermal rectification factor of monolayer triangular GNR indicates that the thermal rectification factor is still as large as 20-30% for a 23 nm long triangular GNR even in the presence of edge roughness.

Acknowledgments

This work is supported by the Semiconductor Research Corporation (SRC) - Nanoelectronics Research Initiative (NRI) via Midwest Institute for Nanoelectronics Discovery (MIND). We thank Dr. Gang Wu (National University of Singapore) for helpful communications on the MD code and Mr. Yaohua Tan (Purdue University) and Prof. Zhigang Jiang (Georgia Tech) for insightful discussions on graphene.

References

1. K. S. Novoselov, A. K. Geim, S. V. Morozov, D. Jiang, Y. Zhang, S. V. Dubonos, I. V. Gregorieva, A. A. Firsov, Science 306, 666 (2004)
2. A. H. Castro Neto, F. Guinea, N. M. R. Peres, K. S. Novoselov, A. K. Geim, Rev. Mod. Phys. 81, 109 (2009)
3. A. A. Balandin, S. Ghosh, W. Bao, I. Calizo, D. Teweldebrhan, F. Miao, C. N. Lau, Nano Lett. 8, 902 (2008)
4. S. Ghosh, I. Calizo, D. Teweldebrhan, E. P. Pokatilov, D. L. Nika, A. A. Balandin, W. Bao, F. Miao, C. N. Lau, Appl. Phys. Lett. 92, 151911 (2008)
5. C. Lee, X. Wei, J. W. Kysar, J. Hone, Science, 321, 385 (2008)
6. Y. W. Son, M. L. Cohen, S. G. Louie, Nature 444, 347 (2006)
7. M. Y. Han, B. Özyilmaz, Y. Zhang, P. Kim, Phys. Rev. Lett. 98, 206805 (2007)
8. J. Hu, X. Ruan, Y. P. Chen, Nano Letters, ASAP (2009)
9. J. Jiang, J. Wang, B. Li, Phys. Rev. B 79, 205418 (2009)
10. N. Yang, G. Zhang, B. Li, arXiv:0906.1046v1 (2009)
11. B. Li, L. Wang, G. Casati, Phys. Rev. Lett. 93, 184301 (2004)
12. B. Li, L. Wang, G. Casati, Appl. Phys. Lett. 88, 143501 (2006)
13. L. Wang, B. Li, Phys. Rev. Lett. 99, 177208 (2007)
14. L. Wang, B. Li, Phys. Rev. Lett. 101, 267203 (2008)
15. D. W. Brenner, Phys. Rev. B 42, 9458 (1990)
16. S. J. Nosé, Chem. Phys. 81, 511 (1984)
17. W. G. Hoover, Phys. Rev. A 31, 1695 (1985)
18. P. H. Hunenberger, Adv. Polym. Sci. 173, 105 (2005)
19. J. Hu, X. Ruan, Z. Jiang and Y. P. Chen, submitted to 2009 TECHCON Conference, Austin TX (2009)